Transplant International

Transplant International ISSN 0934-0874

ORIGINAL ARTICLE

Characteristic immune, apoptosis and inflammatory gene profiles associated with intestinal acute cellular rejection in formalin-fixed paraffin-embedded mucosal biopsies

Tadafumi Asaoka,[1] Eddie R. Island,[1] Panagiotis Tryphonopoulos,[1] Gennaro Selvaggi,[1] Jang Moon,[1] Akin Tekin,[1] Alexandra Amador,[1] David M. Levi,[1] Jennifer Garcia,[2] Leslie Smith,[2] Seigo Nishida,[1] Debbie Weppler,[1] Andreas G. Tzakis[1] and Phillip Ruiz[1]

1 Department of Surgery, University of Miami Miller School of Medicine, Miami, FL, USA
2 Department of Pediatrics, University of Miami Miller School of Medicine, Miami, FL, USA

Keywords
gene signature, human, molecular biomarker, multivisceral transplantation, small bowel transplantation.

Correspondence
Phillip Ruiz MD, PhD, Department of Surgery, 1600 NW, 10th Avenue, Rosensteil Medical Science Building 8150, University of Miami Miller School of Medicine, Miami, FL, 33136, USA. Tel.: +305 243 9616; fax: +305 243 1223; e-mail: pruiz@med.miami.edu

Conflicts of Interest
The authors have declared no conflicts of interest.

Received: 19 November 2010
Revision requested: 1 January 2011
Accepted: 23 March 2011
Published online: 9 May 2011

doi:10.1111/j.1432-2277.2011.01259.x

Summary

Small bowel transplantation (SBT) is becoming a preferred treatment for patients with irreversible intestinal failure. Despite continuous improvement of immunosuppression, SBT is plagued by a high incidence of acute cellular rejection (ACR) that is frequently intractable. Therefore, there is a need for reliable detection markers and novel immunosuppressive strategies that can achieve better control of ACR. We hypothesized that particular transcriptomes provide critical regulation of the intragraft immune response. The aim of our study was to detect potential molecular biomarkers for identifying ACR in minute mucosal biopsies. We examined 30 intestinal mucosal biopsies (AR/NR; 17/13) obtained from recipients after SBT or multivisceral transplantation. We utilized TaqMan® Gene Signature Arrays (immune, inflammation and apoptosis) and investigated the expression of 280 genes. As one of our validations, we performed immunohistochemistry for selected targets. We detected 252 mRNAs in total, 92 of which were found with significantly different expression levels between the AR and NR groups. Immunohistochemistry showed significantly increased staining for IL1R2, ICAM1, GZMB, and CCL3 ($P < 0.05$) during ACR. For the first time, we characterize the potential molecular changes that are associated with modulation of histological appearances of intestinal ACR. These differences in transcriptome patterns can be used to identify robust biomarkers and potential novel therapeutic targets for immunosuppressive agents.

Introduction

Small bowel transplantation (SBT) has become a viable treatment option for patients with irreversible intestinal failure. However, long-term graft survival can often be reduced compared with transplantation of other solid organs. This is largely because of the high complication rates with SBT, notably including acute rejection. The first episode of acute rejection occurs within the first 3 months following transplantation in over 80% of allograft recipients and graft failure secondary to rejection occurs in about 30–40% of transplants [1–3]. Multivisceral transplantation (MVT) is one of the forms of SBT. Previous reports have suggested that the small intestinal allograft (particularly the ileum) is the most susceptible organ to acute cellular rejection (ACR) in frequency and severity when compared with other allografts within the MVT and it has been recognized as the Achilles heel and critical organ of MVT [4]. Therefore, in the management of intestinal graft, the early detection and treatment of ACR is essential.

The recognition and diagnosis of intestinal ACR depends upon clinical observation and histological findings of

endoscopically guided mucosal biopsy specimens. The endoscopic appearance of intestinal ACR ranges from edema and hyperemia in mild cases to granularity, loss of the fine mucosal vascular pattern, diminished peristalsis, and mucosal ulceration in more severe cases. The final diagnosis depends on histological analysis of mucosal biopsy specimens. The histological diagnosis of intestinal ACR is mainly based on a various combination of following features, mixed infiltration of mononuclear cells, crypt injury, and apoptotic bodies in crypt regions [5,6].

Recent advances in genetic information using high throughput microarrays has revealed that there are quite different gene expression patterns associated with rejection status in other types of solid organ transplantation [7–10]. These studies have demonstrated that subtypes of acute rejection (humoral versus cellular) can differ within and between particular organs that have been transplanted. In this regard, bowel transplantation remains with no description to date as to which genes are modified (*in situ*) during the course of acute rejection. A further understanding of the molecular mechanisms of intestinal ACR is essential for identification of new therapeutic targets and ultimately improving graft survival.

We hypothesized that small bowel allografts undergoing ACR show distinct gene expression profiles that reflect the histopathological changes in bowel biopsies. The aim of this study was to characterize the potential molecular changes of intestinal grafts undergoing alloreactive inflammation to identify involved molecular pathways.

Materials and methods

Study sites and internal review board (IRB) approval

This study was performed at the University of Miami, Miami Transplant Institute. The Internal Review Board of the University of Miami approved the study protocol.

Patients and controls

A total of 295 patients underwent small bowel or multivisceral transplantation in our institute from August 1994 to October 2010. Out of the intestinal biopsy samples from those patients, a total of 60 cases of intestinal mucosal biopsy specimens from 55 recipients after SBT and multivisceral transplantation were available for this study. The tissue was preserved in 10% buffered formalin and routinely processed. Hematoxylin and eosin (H&E)-stained sections of the biopsy samples were examined by a pathologist who was blinded to the results of the molecular studies. Histopathological assessments were performed with special concern to ACR in each graft. In analysis pertaining to ACR, these rejection grades were evaluated based on the previously established grading schema in small intestinal transplantation [5,11]. None of the chosen biopsies had morphological or clinical evidence of concomitant infection, post-transplant lymphoproliferative disease (PTLD) or other complications. All biopsies were performed by clinical indication or follow up, using endoscopy. All patients' diagnosis of intestinal ACR was pathologically confirmed and the clinical course followed up after treatment. After clinicopathological evaluation, we evaluated all formalin-fixed paraffin-embedded (FFPE) biopsy samples for the gene signature assays or immunohistochemical staining. These were divided into two groups, AR (acute cellular rejection, mild or greater grade) and NR (histologically, no evidence of acute rejection or indeterminate for acute rejection) group based on clinicopathological features. A total of 25 normal intestinal tissue specimens from explanted small bowel tissues were pooled and used as the reference of gene signature assay.

RNA isolation

Total RNA was extracted from FFPE biopsy samples using RecoverAll™ Total Nucleic Acid Isolation Kit (Applied Biosystems, Foster City, CA, USA) for FFPE Tissues according to the manufacturer's instructions. The concentration and quality of total RNA were measured by a NanoDrop ND-1000 spectrophotometer (Nanodrop Technologies, Wilmington, DE, USA) and checked by the UV absorbance at 260 nm and 280 nm ($A_{260/280}$).

Gene signature assays

We utilized a Real-time PCR based TaqMan Low Density Array (TLDA) containing 92 assays associated with each target pathway (immune, inflammation and apoptosis) and four assays of endogenous control (Applied Biosystems). Total RNA (60 ng) was reverse transcribed using TaqMan Random RT Primers. Next, an optional amplification step can be performed using Megaplex™ PreAmp Primers (Applied Biosystems, Foster City, CA, USA). For the final quantitation step, TaqMan® Universal PCR Master Mix (Applied Biosystems, Foster City, CA, USA) is added to each sample and the mixtures are pipetted into the panel. The real-time PCR is run on the Applied Biosystems 7900HT Fast Real-Time PCR System.

Analysis of PCR-array data

Data analysis was performed by SDS software and baseline and threshold were automatically set. Expression data were normalized using GAPDH as the endogenous control and relative quantification was performed based on pooled normal intestines using a comparative Ct method.

Several target mRNAs that had Ct values >35 were eliminated from analysis. Messenger RNAs with missing values in more than 20% of cases were excluded from further analysis. The data were analyzed with Significance Analysis of Microarray (SAM) [12] which utilized repeated permutations of the data to determine if the expressions of any genes are significantly related to the response. The expression patterns were visualized with Cluster 3.0 (http://bonsai.ims.utokyo.ac.jp/~mdehoon/software/cluster/software.htm#ctv) and Java Tree View software (http://sourceforge.net/projects/jtreeview) (Eisen Lab, Stanford, CA, USA), using average linkage and Spearman rank correlation as a measurement for similarity. As a classification method between two classes, we adopted a weighted voting (WV) algorithm, generally used in gene expression profiling [13–15].

Immunohistochemical Staining

Formalin-fixed paraffin-embedded small intestinal mucosal biopsy specimens were stained with monoclonal antibody using an indirect diaminobenzidine (DAB) technique. All samples were fixed with 10% neutral buffered formalin for several hours, and embedded in the paraffin block. The sections of 4 μm in thickness from each block were prepared for immunohistochemical staining. Deparaffinization and rehydration of sections were performed using xylene and ethanol. Endogenous peroxidase activity was blocked by nonhydrogen peroxide formula (PeroxAbolish; Biocare Medical, Concord, CA, USA). Antigen retrieval was performed using a pressure cooker at 120 °C for 10 min, soaking sections in an antigen retrieval solution, Borg Decloaker (Biocare Medical, Concord, CA, USA) of pH 9.5. After blocking nonspecific biding with blocking reagent (normal horse serum) for 20 min, the sections were incubated with primary antibody. Rabbit anti-Human IL1R2 Polyclonal Antibody (Novus Biologicals, Littleton, CO, USA), Rabbit anti-Human GZMB Polyclonal Antibody (Abcam, IHC, Cambridge, MA, USA), Rabbit anti-Human ICAM1 Monoclonal Antibody (Abcam, IHC), Rabbit anti-Human IL10 Polyclonal Antibody (Abcam, IHC) and Goat anti-Human MIP-1α Polyclonal Antibody (Santa Cruz Biotechnology, Inc., Santa Cruz, CA, USA) were added at appropriate dilutions overnight at 4 °C. The sections were washed and incubated with polymer horse radish peroxidase (HRP) conjugated anti-rabbit or goat secondary antibody (Vector Laboratories, Burlingame, CA, USA) for 40 min at room temperature, then, washed and incubated with diaminobenzidine tetrahydrochloride (DAB; Vector Laboratories), and counterstained with hematoxylin. The negative control was prepared in the same manner except that the primary antibody was omitted.

Microscopic analysis

The total area of all stained sections was examined and the expression levels of IL1R2, ICAM1, and IL-10 were scored independently by two observers including an experienced pathologist. Samples were coded in such a way as to ensure blind scoring. Semiquantitative scoring was performed separately on a 4-point scale. A score of 0 represented absence of staining; 1 indicates very low density of positive cells; 2 and 3 indicates a moderate and highest density of positive cells, respectively. A similar score was assigned to the expression of each molecule on microvessel endothelium and infiltrating cells. Individual readings were identical or differed by only one point. Minor differences between the observers were resolved by mutual agreement. To evaluate the immunopositive cells for CCL3 and GZMB, representative areas of each tissue section were selected, and positive cells were counted in at least three fields (×40) in these area. Two observers performed semiquantitation and the average number of positive cells in one view was calculated.

Statistical analysis

Data were expressed as median and range values. Differences were tested by the exact chi-square test or Mann–Whitney *U*-test. All differences were considered statistically significant at a P-value <0.05.

Results

Clinicopathological features of transplant recipients

Of 60 intestinal mucosal biopsy specimens from 55 patients, 30 samples from 25 patients after SBT or MVT were nominated to gene signature assays and 30 samples from additional 30 patients were enrolled to the validation by immunohistochemical staining. Of 60 (65%) biopsies, 39 were from patients after MVT (stomach, pancreaticoduodenal complex, and intestine, with liver) or modified MVT (without liver). In 51 of 60 biopsies (85%), tacrolimus was administered as the basal immunosuppressant with steroids at diagnosis. Twenty-nine of 60 biopsy specimens (48%) showed histological evidence of ACR that required rejection treatment. All patients of the AR group received rejection therapy or the dose of maintenance immunosuppression was increased and 22 of 29 patients in the AR group showed recovery, but in seven cases, rejected intestinal allografts were eventually removed. Typically, intestinal ACR with more than grade 2 were selected as AR group for gene signature assays. The clinical characteristics of the cases that underwent gene signature assays (n = 30) and immunohistochemical

Table 1. Clinical characteristics of patients at diagnosis in (a) gene signature assay samples and (b) immunohistochemical staining samples.

(a) Gene signature assay samples

Category	Variables	NR (n = 13)	AR (n = 17)	P-value
Recipient age (years)		3 (0.9–65)	9 (1–49)	NS
Recipient gender	M/F	8/5	11/6	NS
Donor age (years)		3 (0.1–28)	3 (0.2–40)	NS
Donor gender	M/F	8/5	5/12	NS
Postoperative day (day)		166 (62–2084)	302 (8–2577)	NS
Immune suppression	FK	2	1	NS
	FK/steroid	11	16	
	Rapamycin addition	0	3	
Rejection grade	No evidence of rejection	11	0	
	Indeterminate	2	0	
	Mild	0	0	
	Moderate	0	8	
	Severe	0	9	
Graft	Isolated intestine	4	6	NS
	MVT/MMVT	9	11	

(b) Immunohistochemical staining samples

Category	Variables	NR (n = 18)	AR (n = 12)	P-value
Recipient age (years)		28 (1–57)	21 (2–66)	NS
Recipient gender	M/F	9/9	5/7	NS
Donor age (years)		7 (0–23)	7 (1–21)	NS
Donor gender	M/F	10/8	7/5	NS
Postoperative day (day)		94 (3–3822)	444 (18–3243)	NS
Immune suppression	FK	6	0	0.04
	FK/steroid	12	12	
	Rapamycin addition	0	1	
Rejection grade	No evidence of rejection	14	0	
	Indeterminate	4	0	
	Mild	0	4	
	Moderate	0	4	
	Severe	0	4	
Graft	Isolated intestine	6	6	NS
	MVT/MMVT	12	6	

MMVT, modified multivisceral transplantation; NS, nonsignificant.

staining (n = 30) studies are summarized in Table 1a and b.

Selection of mRNA marker candidates for intestinal ACR

After conducting SAM analysis with the 1000 permutation test, 92 of 252 genes were selected as differentially expressed genes among the groups, with a false discovery rate of 8.72%. Supervised clustering of these genes revealed distinct expression patterns between the AR and NR groups (Fig. 1).

Next, we examined the accuracy of ACR diagnosis using these 92 genes based on the WV algorithm with a leave-one-out cross-validation approach (Figure S1). Using all 92 genes for classification, 25 of 30 cases (83.3%) were correctly classified to either the AR or NR group (Figure S2).

Immunohistochemical results

Thirty biopsy specimens from 30 intestinal transplant recipients were studied. Twelve of thirty allograft cases showed evidence of histological ACR (mild/moderate/severe, 4/4/4). Eighteen of thirty cases showed no evidence of rejection (n = 14) or were indeterminate for rejection (n = 4). We selected the five targets (IL1R2, GZMB, ICAM1, IL10, and CCL3) to validate our RT-PCR array results. All of the proteins had a tendency for increased expression in the AR group. During intestinal ACR, IL1R2, GZMB, and IL-10 producing

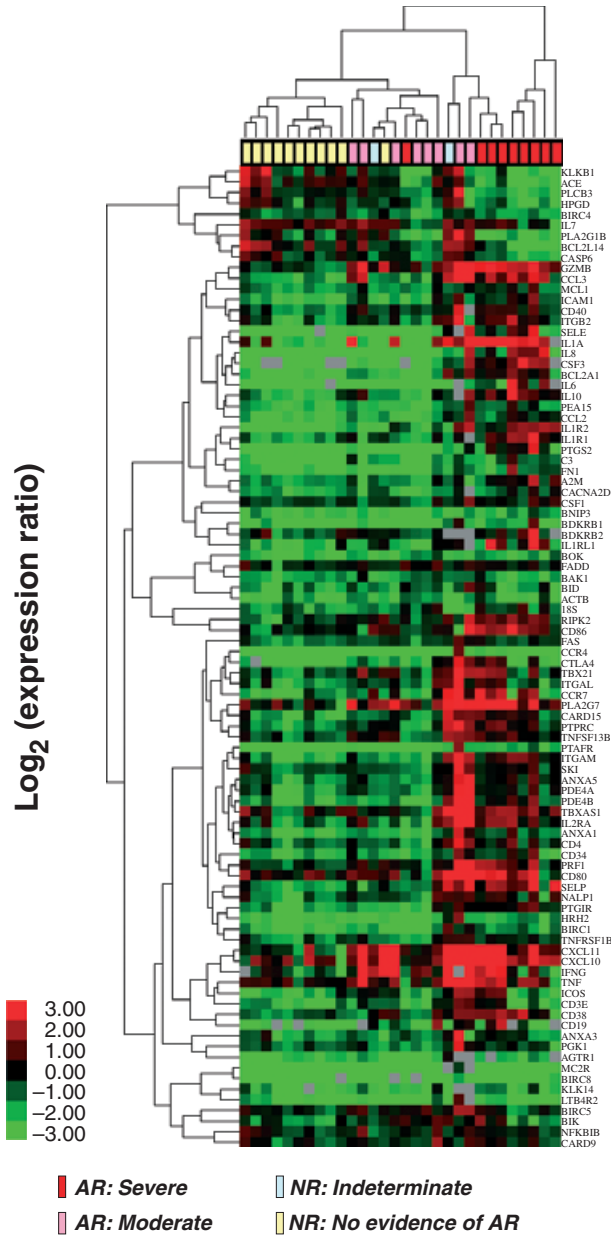

Figure 1 Hierarchical clustering with 92 selected genes. Hierarchical clustering with 92 selected genes. The rows and columns represent genes and samples, respectively. The color bar indicates the relative expression levels.

mononuclear cells highly infiltrated the allografts (Fig. 2 a, c, and i).

Immunohistochemical localization for IL-10 and IL1R2 was detected in the surface epithelium and lamina propria mononuclear cells. Most of the rejection cases had more extensive epithelium staining and positive mononuclear cell infiltration. However, there were no significant differences in the semiquantitative score for IL-10 between AR and NR group.

The expression of ICAM1 and CCL3 proteins was increased during intestinal ACR and mainly observed on the surface of vascular endothelium and infiltrating macrophages respectively (Fig. 2e and g). By comparison, most of the allografts without ACR showed only weak and basal expression of these selected proteins (Fig. 2b, d, f, h, and j). The positive staining of IL1R2, ICAM1, GZMB, and CCL3 proteins was significantly correlated to the development of intestinal ACR ($P < 0.05$) (Fig. 3). These differences in protein intensity served as a validation of the microarray data for these genes.

Discussion

Our data demonstrate that we successfully characterized distinct intragraft gene expression patterns for immune, inflammatory and apoptotic genes associable with intestinal ACR in FFPE intestinal mucosal biopsies. We comprehensively examined the expression of 280 genes associated with the aforementioned pathways and established consistent, reproducible molecular pathway changes occurring during intestinal allograft rejection.

Our molecular signature for intestinal ACR demonstrated a relative overexpression of various leukocyte surface markers including CD3E, CD4 (T cell), and CD19 (B cell) as well as CD34 (hematopoietic progenitor cells), CD80, and CD86 (dendritic-cells/macrophages) (Table 2). One of the foremost histological features of intestinal ACR is infiltration by a mixed but primarily mononuclear inflammatory population including blastic or activated lymphocytes [5,11]. The overexpression of these molecules appears to correlate with mixed infiltration. As important signals to induce macrophages and lymphocytes infiltration, we also detected several chemokines in our study. Monocyte chemotactic peptide-1 (MCP-1/CCL2) is an essential chemotactic and activating factor for monocytes and macrophages [16]. Macrophage inflammatory protein-1 alpha (CCL3/MIP-1α) is also important for leukocyte recruitment [17]. The significant overexpression of CCL2, CCL3 and the binding receptor CCR4 is likely to suggest their significant role in the accumulation of macrophages and lymphocytes in bowel allografts [18].

Dendritic cells and macrophages are professional antigen presenting cells (APCs) and present antigen to T cells efficiently, however, the antigen-specific signal generated by the T-cell receptor (TCR) is generally insufficient for optimal T-cell activation [19]. The full activation of allograft-specific T lymphocytes simultaneously requires the expression of co-stimulatory signals such as CD40, ICOS, CD80, CD86, and CTLA4. For example, CD40 is a co-stimulatory protein found on APCs and is required for their activation. In the macrophage, the primary signal for activation is IFN-γ from Th1 type CD4 T cells. The

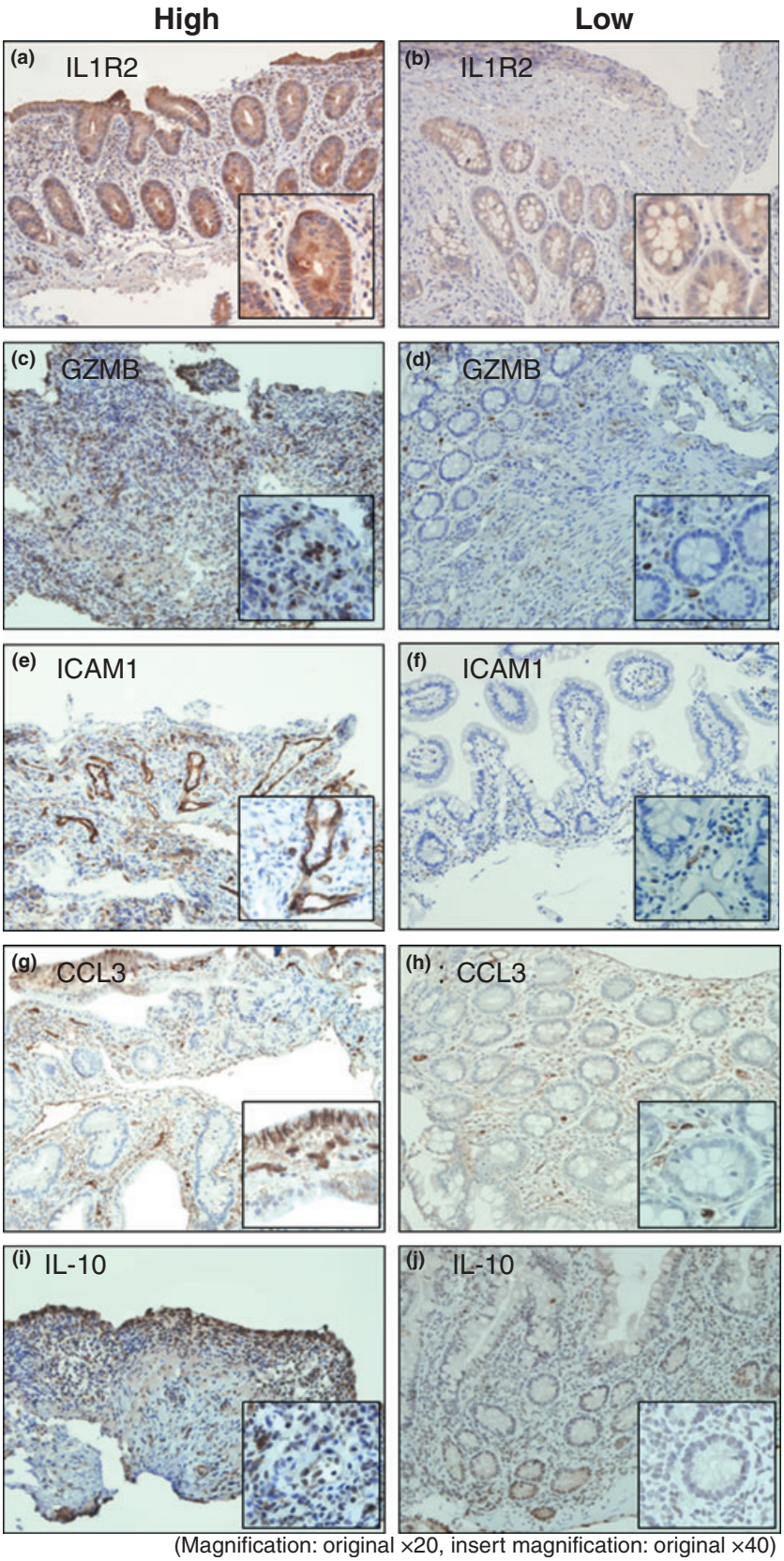

Figure 2 Protein expression and distribution in ileum biopsy specimens. Immunohistochemical staining for IL1R2, GZMB, ICAM1, CCL3, and IL-10 were performed to validate microarray results. During intestinal ACR, IL1R2, GZMB, and IL-10 producing mononuclear cells highly infiltrated to the allograft (a, c, and i). The expression of ICAM1 and CCL3 protein was increased during intestinal ACR and mainly observed on the surface of vascular endothelium and infiltrating macrophages respectively (e, g). But most of the allografts without ACR showed the only weak and basal expression of these selected proteins (b, d, f, h, and j). (Magnification: original ×20, Insert magnification: original ×40)

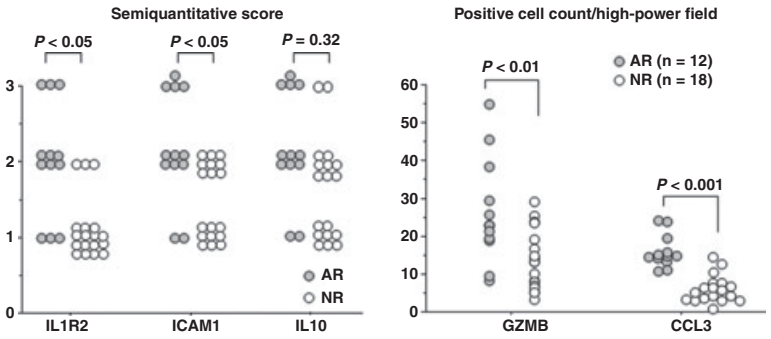

Figure 3 Semiquantification of immunohistochemistry. Differences of each semiquantitative score and positive cell count were tested by the exact chi-square test or Mann–Whitney *U*-test between AR (n = 12) and NR group (n = 18).

secondary signal is CD40L (CD154) on the T cell that binds CD40 on the macrophage cell surface. As a result, the macrophage expresses more CD40 and TNF receptors on its surface which helps increase the level of activation [19]. Actually, several studies demonstrated the blockade of co-stimulatory signals induces prolonged graft survival in animal models [20,21]. Our findings support that the distinct overexpression of CD40 mRNA in the intestinal allograft likely reflects the infiltration of activated APCs critical for initiation and sustainment of the alloimmune response; moreover, these molecules could serve as molecular markers and treatment target for intestinal rejection.

We simultaneously characterized CD4 subtype distribution in intestinal ACR at the level of mRNA (Fig. 4). The overexpression of Th1- associated molecules (T-bet, GZMB, and IFNγ) appeared to demonstrate the imbalance of CD4 subtype infiltration in allografts during intestinal ACR. Th1 predominant infiltration promotes cytotoxic T lymphocyte (CTLs) activation and GZMB/Perforin-mediated graft injury is induced by CTL activation.

Several studies have reported increased apoptosis in other solid organ transplants with ACR [22–26]. GZMB/PFR1 pathways are the main mechanisms by which CTLs induce cell death and act together to induce endothelial cell death in allografts [27]. GZMB and PFR1 are the most extensively studied granzymes that induce cell death through the activation of caspase-dependent and independent pathways [28]. The overexpression of Fas and FADD mRNA suggested that the Fas/Fas ligand pathway was also an alternative mechanism for mediating graft injury [29], although, in our results, there was no significant up-regulation in the expression of Caspase 1-10 during intestinal ACR. In situations in which caspase activity is blocked, GZMB can directly cleave and inactivate proteins involved in cellular structure and function, and contribute to the dismantling of target cells [30]. It might be that CTLs induce cell death of allogenic endothelial cells and crypt cells predominantly through a caspase-independent mechanism in intestinal allografts.

Vascular endothelial cells are important main targets of CTLs in all solid organ allografts [25]. The significant overexpression of Intercellular adhesion molecule-1 (ICAM1) and E-selectin, which are adhesion molecules and expressed on activated endothelium, is compatible with the premise that vascular endothelium, as with other solid organ allografts, serves as powerful target for immune effector cells and molecules. By immunohistochemistry, the high expression of ICAM1 was observed on the surface of venular endothelial cells and several infiltrating cells in allograft with ACR. This finding was distinctly different from that of normal allografts. ICAM1 might serve as a useful biomarker candidate of intestinal ACR.

Interestingly, regulatory T (Treg) cell-associated molecules such as CTLA4 and IL-10 were also up regulated during intestinal ACR and simultaneously, we detected the overexpression of IL1R1 and IL1R2, which are soluble receptor antagonists for IL-1 [31]. These molecules have a natural role in anti-inflammation to suppress the immune response [31,32]. Our results imply that these molecules aid in stabilizing inflammation within the graft and might reflect an attempt at neutralization of host defenses within the rejecting graft milieu. In our immunohistochemical staining for IL-10, there was not a significant difference between AR and NR. It might be difficult to discriminate AR from NR based on this staining result, because the protein encoded by this gene is expressed in several infiltrating cells and the intestinal mucosa is one of the tissues in which a large number of immune cells reside. Actually, there were many positive cells for this protein (data not shown) in the normal intestine. An understanding of the ratio of this immunoregulatory molecule may also be valuable in assessing inflamed grafts that are clinically stable (typically later in the transplant course); it could be that host regulation processes are preventing parenchymal injury of coexisting inflammatory cells.

Complement component C3 plays a central role in the activation of complement system. Its activation is required for antibody-mediated rejection (AMR) in organ transplantation. In addition, recent studies have demon-

Table 2. Genes most frequently included in the significance analysis of microarray (SAM) classifier.

Positive genes (83)			
Gene symbol	Gene name	Fold change[1]	FDR (%)
IL1R2	Interleukin 1 receptor, type II	28.4	0.0
CD40	CD40 molecule	3.5	0.0
GZMB	Granzyme B	6.0	0.0
ICAM1	Intercellular adhesion molecule 1	4.3	0.0
CCR4	Chemokine (C-C motif) receptor 4	11.7	0.0
IL8	Interleukin 8	45.5	0.0
CCL3	Chemokine (C-C motif) ligand 3	9.8	0.0
IL10	Interleukin 10	6.0	0.0
PTAFR	Platelet-activating factor receptor	5.7	0.0
SELE	Selectin E (endothelial adhesion molecule 1)	12.2	0.0
IL1A	Interleukin 1, alpha	15.7	0.0
CXCL11	Chemokine (C-X-C motif) ligand 11	9.1	0.0
CSF3	Colony stimulating factor 3	18.3	0.0
BCL2A1	BCL2-related protein A1	3.1	0.0
PLA2G7	Phospholipase A2, group VII	3.6	0.0
ANXA5	Annexin A5	4.8	0.0
ITGAM	Integrin, alpha M	3.7	0.0
SELP	Selectin P	3.7	0.0
C3	Complement component 3	3.8	0.0
CTLA4	Cytotoxic T-lymphocyte-associated protein 4	5.6	0.0
IL1R1	Interleukin 1 receptor, type I	4.3	0.0
MCL1	Myeloid cell leukemia sequence 1 (BCL2-related)	2.1	0.0
PRF1	Perforin 1	4.4	0.0
BOK	BCL2-related ovarian killer	1.9	0.0
FADD	Fas (TNFRSF6)-associated via death domain	1.4	0.0
FAS	Fas	1.7	0.0
CARD15	Nucleotide-binding oligomerization domain containing 2	1.4	0.0
MC2R	Melanocortin 2 receptor	2.0	0.0
PDE4A	Phosphodiesterase 4A, cAMP-specific	5.3	0.0
KLK14	Kallikrein-related peptidase 14	2.4	0.0
ANXA1	Annexin A1	3.5	0.0
PTGIR	Prostaglandin I2 (prostacyclin) receptor (IP)	3.2	0.0
PTGS2	Prostaglandin-endoperoxide synthase 2	14.8	0.0
CCL2	Chemokine (C-C motif) ligand 2	2.9	0.0
BIRC8	Baculoviral IAP repeat-containing 8	3.4	0.0
CXCL10	Chemokine (C-X-C motif) ligand 10	4.8	0.0
IL2RA	Interleukin 2 receptor, alpha	5.6	0.0
ITGB2	Integrin, beta 2	2.8	0.0
FN1	Fibronectin 1	4.1	0.0
IL6	Interleukin 6	37.9	1.3
NALP1	NLR family, pyrin domain containing 1	1.9	1.3
CD34	CD34 molecule	3.3	1.3
PDE4B	Phosphodiesterase 4B, cAMP-specific	9.2	1.3
TBX21	T-box 21	4.0	1.3
RIPK2	Receptor-interacting serine-threonine kinase 2	2.0	1.3
PEA15	Phosphoprotein enriched in astrocytes 15	2.3	1.3
18S	18S	2.1	1.3
CCR7	Chemokine (C-C motif) receptor 7	2.7	2.3
ITGAL	Integrin, alpha L	2.2	2.3
TNF	Tumor necrosis factor	2.3	2.3
BID	BH3 interacting domain death agonist	2.2	2.3
CD19	CD19 molecule	5.1	2.3
A2M	Alpha-2-macroglobulin	2.8	3.0
CSF1	Colony stimulating factor 1 (macrophage)	1.6	3.0
CD38	CD38 molecule	2.7	3.4

Table 2. continued

Positive genes (83)			
Gene symbol	Gene name	Fold change[1]	FDR (%)
BDKRB1	Bradykinin receptor B1	3.2	3.8
BIRC5	Baculoviral IAP repeat-containing 5 (survivin)	1.7	3.8
ACTB	Actin, beta	1.9	3.8
NFKBIB	Nuclear factor of kappa light polypeptide gene enhancer in B cells inhibitor, beta	1.3	3.8
PTPRC	Protein tyrosine phosphatase, receptor type, C	1.8	3.8
BDKRB2	Bradykinin receptor B2	2.9	5.0
BIRC1	NLR family, apoptosis inhibitory protein	1.1	5.0
CD3E	CD3e molecule, epsilon (CD3–TCR complex)	2.3	5.0
ANXA3	Annexin A3	2.5	5.0
BIK	BCL2-interacting killer (apoptosis-inducing)	1.6	5.0
IL1RL1	Interleukin 1 receptor-like 1	5.1	5.0
TNFSF13B	Tumor necrosis factor (ligand) superfamily, member 13b	1.3	5.0
BNIP3	BCL2/adenovirus E1B 19 kDa interacting protein 3	1.5	6.2
CD86	CD86 molecule	2.7	6.2
TBXAS1	Thromboxane A synthase 1 (platelet, cytochrome P450, family 5, subfamily A)	2.9	6.2
TNFRSF1B	Tumor necrosis factor receptor superfamily, member 1B	1.4	6.2
ICOS	Inducible T-cell co-stimulator	2.6	6.2
LTB4R2	Leukotriene B4 receptor 2	2.2	6.5
SKI	v-ski sarcoma viral oncogene homolog (avian)	1.9	6.5
BAK1	BCL2-antagonist/killer 1	1.5	6.5
CD80	CD80 molecule	3.6	6.5
CARD9	Caspase recruitment domain family, member 9	1.4	6.5
CD4	CD4 molecule	2.0	6.5
PGK1	Phosphoglycerate kinase 1	1.9	7.5
AGTR1	Angiotensin II receptor, type 1	1.5	7.5
HRH2	Histamine receptor H2	2.2	7.5
IFNG	Interferon, gamma	2.6	7.5
CACNA2D1	Calcium channel, voltage-dependent, alpha 2/delta subunit 1	1.9	8.7
Negative genes (9)			
Gene ID			
KLKB1	Kallikrein B, plasma (Fletcher factor) 1	0.3	1.3
PLCB3	Phospholipase C, beta 3	0.8	1.3
BIRC4	Baculoviral IAP repeat-containing 4	0.5	1.3
ACE	Angiotensin I converting enzyme (peptidyl-dipeptidase A) 1	0.4	3.0
HPGD	Hydroxyprostaglandin dehydrogenase 15-(NAD)	0.5	3.0
PLA2G1B	Phospholipase A2, group IB (pancreas)	0.7	3.0
BCL2L14	BCL2-like 14 (apoptosis facilitator)	0.4	3.0
IL7	Interleukin 7	0.6	3.0
CASP6	Caspase 6, apoptosis-related cysteine peptidase	0.5	3.8

[1]Fold change means relative fold, AR (median)/NR (median).
FDR, false discovery rate.

strated that the complement system participates in the regulation of T-cell functions by multiple mechanisms such as the direct opsonization of foreign antigens [33,34]. Hepatocytes are the primary source of complement components, but it has been suggested that locally biosynthesized complement in the intestine might contribute to immune and inflammatory responses [35]. The significant overexpression of C3 mRNA during intestinal

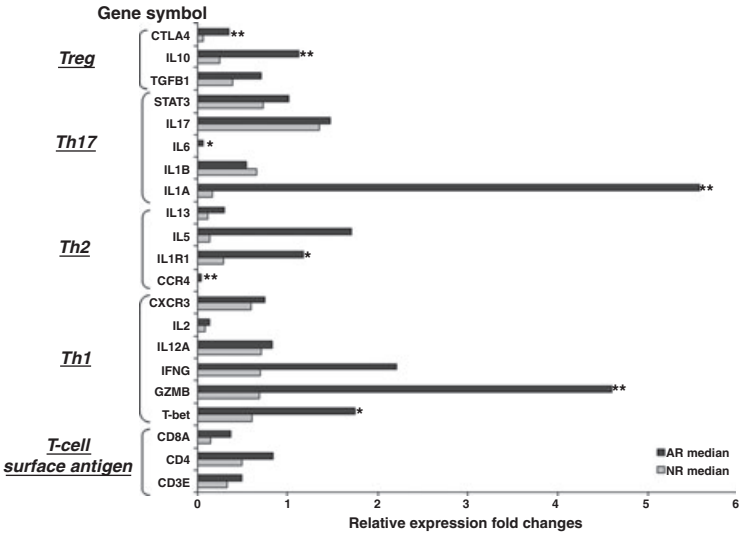

Figure 4 CD4 subtype distribution in small bowel grafts. T-bet, GZMB, IL6, IL1A, IL1R1, CTLA4, IL10, and CCR4 were significantly overexpressed during intestinal ACR. These overexpression profiles revealed the predominant activation of Th1, Th17, and Treg at the level of the transcriptome. The relative expression of each sample was calculated using the expression level of normal ileum mixture as a reference (Mann–Whitney *U*-test; $**P < 0.01$, $*P < 0.05$).

ACR is likely associated with acute rejection and the fact that clinical intestinal transplantation is plagued by a high incidence of intractable rejection.

Generally, when studying gene expression in clinical environments, the heterogeneity of graft specimens like gender, age, comorbidity and medications complicates conclusions regarding the underlying mechanism of rejection. Furthermore, high throughput microarrays are susceptible to noise because of their limited dynamic range compared with real-time PCR [36]. However, we used the real-time PCR based array focusing on immune, inflammatory and apoptosis. The definition of new transcriptome sets based directly on human biopsies may provide further enhancement of this methodology.

One of the limitations of this study is the sample selection for gene signature assay. We selected the rejection cases with more than grade 2 to investigate the most typical gene expression differences. However, it is clinically needed to detect the early onset of rejection unrecognized by histological features. Further evaluation in low-grade rejection cases will be needed.

In conclusion, this study has demonstrated for the first time that small bowel allografts undergoing ACR show different gene expression profiles from that of normal intestinal allografts in FFPE mucosal biopsies. Our study provides novel insights into immune, apoptosis and inflammatory pathways operative in small bowel transplantation.

Authorship

TA: performed research and participated in the study design, writing the paper, and data analysis. ERI, PT, GS, JM, AT, AA, DML, and JG: participated in obtaining clinical data. LS, SN, DW, and AGT: participated in the study design and suggestions. PR: participated in the study design, revising the paper, pathological diagnosis and data analysis.

Funding

The authors have declared no funding.

Acknowledgements

The authors wish to thank Dayami Hernandez for her excellent histological expertise, and Jennifer McCue and Irvana Eloundou-Avomo for their technical expertise.

Supporting Information

Additional Supporting Information may be found in the online version of this article:

Figure S1 Accuracy curve using weighted voting algorithm.

Figure S2 Prediction value of acute cellular rejection.

Please note: Wiley-Blackwell are not responsible for the content or functionality of any supporting materials supplied by the authors. Any queries (other than missing material) should be directed to the corresponding author for the article.

References

1. Fishbein TM, Gondolesi GE, Kaufman SS. Intestinal transplantation for gut failure. *Gastroenterology* 2003; **124**: 1615.
2. Selvaggi G, Gaynor JJ, Moon J, *et al.* Analysis of acute cellular rejection episodes in recipients of primary intestinal transplantation: a single center, 11-year experience. *Am J Transplant* 2007; **7**: 1249.

3. Kato T, Ruiz P, Thompson JF, *et al.* Intestinal and multivisceral transplantation. *World J Surg* 2002; **26**: 226.
4. Takahashi H, Kato T, Delacruz V, *et al.* Analysis of acute and chronic rejection in multiple organ allografts from retransplantation and autopsy cases of multivisceral transplantation. *Transplantation* 2008; **85**: 1610.
5. Ruiz P, Bagni A, Brown R, *et al.* Histological criteria for the identification of acute cellular rejection in human small bowel allografts: results of the pathology workshop at the VIII International Small Bowel Transplant Symposium. *Transplant Proc* 2004; **36**: 335.
6. Wu T, Abu-Elmagd K, Bond G, Nalesnik MA, Randhawa P, Demetris AJ. A schema for histologic grading of small intestine allograft acute rejection. *Transplantation* 2003; **75**: 1241.
7. Sarwal M, Chua MS, Kambham N, *et al.* Molecular heterogeneity in acute renal allograft rejection identified by DNA microarray profiling. *N Engl J Med* 2003; **349**: 125.
8. Lande JD, Patil J, Li N, Berryman TR, King RA, Hertz MI. Novel insights into lung transplant rejection by microarray analysis. *Proc Am Thorac Soc* 2007; **4**: 44.
9. Mueller TF, Einecke G, Reeve J, *et al.* Microarray analysis of rejection in human kidney transplants using pathogenesis-based transcript sets. *Am J Transplant* 2007; **7**: 2712.
10. Asaoka T, Kato T, Marubashi S, *et al.* Differential transcriptome patterns for acute cellular rejection in recipients with recurrent hepatitis C after liver transplantation. *Liver Transpl* 2009; **15**: 1738.
11. Lee RG, Nakamura K, Tsamandas AC, *et al.* Pathology of human intestinal transplantation. *Gastroenterology* 1996; **110**: 1820.
12. Tusher VG, Tibshirani R, Chu G. Significance analysis of microarrays applied to the ionizing radiation response. *Proc Natl Acad Sci USA* 2001; **98**: 5116.
13. Golub TR, Slonim DK, Tamayo P, *et al.* Molecular classification of cancer: class discovery and class prediction by gene expression monitoring. *Science* 1999; **286**: 531.
14. Pomeroy SL, Tamayo P, Gaasenbeek M, *et al.* Prediction of central nervous system embryonal tumour outcome based on gene expression. *Nature* 2002; **415**: 436.
15. Ramaswamy S, Ross KN, Lander ES, Golub TR. A molecular signature of metastasis in primary solid tumors. *Nat Genet* 2003; **33**: 49.
16. Segerer S, Nelson PJ, Schlondorff D. Chemokines, chemokine receptors, and renal disease: from basic science to pathophysiologic and therapeutic studies. *J Am Soc Nephrol* 2000; **11**: 152.
17. Cook DN, Beck MA, Coffman TM, *et al.* Requirement of MIP-1 alpha for an inflammatory response to viral infection. *Science* 1995; **269**: 1583.
18. Magil AB. Monocytes/macrophages in renal allograft rejection. *Transplant Rev (Orlando)* 2009; **23**: 199.
19. Rothstein DM, Sayegh MH. T-cell costimulatory pathways in allograft rejection and tolerance. *Immunol Rev* 2003; **196**: 85.
20. Kirk AD, Burkly LC, Batty DS, *et al.* Treatment with humanized monoclonal antibody against CD154 prevents acute renal allograft rejection in nonhuman primates. *Nat Med* 1999; **5**: 686.
21. Kunzendorf U. Co-stimulatory signals during recognition of allo-antigens. *Kidney Blood Press Res* 2000; **23**: 175.
22. Clement MV, Haddad P, Soulie A, *et al.* Perforin and granzyme B as markers for acute rejection in heart transplantation. *Int Immunol* 1991; **3**: 1175.
23. Legros-Maida S, Soulie A, Benvenuti C, *et al.* Granzyme B and perforin can be used as predictive markers of acute rejection in heart transplantation. *Eur J Immunol* 1994; **24**: 229.
24. Li B, Hartono C, Ding R, *et al.* Noninvasive diagnosis of renal-allograft rejection by measurement of messenger RNA for perforin and granzyme B in urine. *N Engl J Med* 2001; **344**: 947.
25. Choy JC, Wang Y, Tellides G, Pober JS. Induction of inducible NO synthase in bystander human T cells increases allogeneic responses in the vasculature. *Proc Natl Acad Sci USA* 2007; **104**: 1313.
26. D'Errico A, Corti B, Pinna AD, *et al.* Granzyme B and perforin as predictive markers for acute rejection in human intestinal transplantation. *Transplant Proc* 2003; **35**: 3061.
27. Choy JC. Granzymes and perforin in solid organ transplant rejection. *Cell Death Differ* 2010; **17**: 567.
28. Sutton VR, Davis JE, Cancilla M, *et al.* Initiation of apoptosis by granzyme B requires direct cleavage of bid, but not direct granzyme B-mediated caspase activation. *J Exp Med* 2000; **192**: 1403.
29. Graziotto R, Del Prete D, Rigotti P, *et al.* Perforin, Granzyme B, and fas ligand for molecular diagnosis of acute renal-allograft rejection: analyses on serial biopsies suggest methodological issues. *Transplantation* 2006; **81**: 1125.
30. Zhang D, Beresford PJ, Greenberg AH, Lieberman J. Granzymes A and B directly cleave lamins and disrupt the nuclear lamina during granule-mediated cytolysis. *Proc Natl Acad Sci USA* 2001; **98**: 5746.
31. Conti F, Breton S, Batteux F, *et al.* Defective interleukin-1 receptor antagonist production is associated with resistance of acute liver graft rejection to steroid therapy. *Am J Pathol* 2000; **157**: 1685.
32. Alegre ML, Frauwirth KA, Thompson CB. T-cell regulation by CD28 and CTLA-4. *Nat Rev Immunol* 2001; **1**: 220.
33. Longhi MP, Harris CL, Morgan BP, Gallimore A. Holding T cells in check – a new role for complement regulators? *Trends Immunol* 2006; **27**: 102.
34. Carroll MC. The complement system in regulation of adaptive immunity. *Nat Immunol* 2004; **5**: 981.
35. Sugihara T, Kobori A, Imaeda H, *et al.* The increased mucosal mRNA expressions of complement C3 and interleukin-17 in inflammatory bowel disease. *Clin Exp Immunol* 2010; **160**: 386.
36. Khatri P, Sarwal MM. Using gene arrays in diagnosis of rejection. *Curr Opin Organ Transplant* 2009; **14**: 34.